# Accepted Manuscript

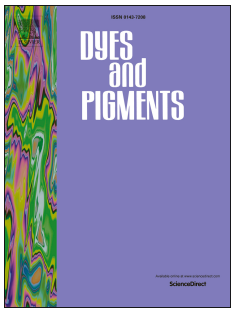


(Bi)phenyl substituted 9-(2,2-diphenylvinyl)carbazoles as low cost hole transporting materials for efficient red PhOLEDs

Saulius Grigalevicius, Daiva Tavgeniene, Gintare Krucaite, Raimonda Griniene, Yen-Po Wang, Shang-Ru Tsai, Chih-Hao Chang

PII: S0143-7208(18)31028-3

DOI: 10.1016/j.dyepig.2018.06.019

Reference: DYPI 6824

To appear in: *Dyes and Pigments*

Received Date: 7 May 2018

Revised Date: 11 June 2018

Accepted Date: 12 June 2018

Please cite this article as: Grigalevicius S, Tavgeniene D, Krucaite G, Griniene R, Wang Y-P, Tsai S-R, Chang C-H, (Bi)phenyl substituted 9-(2,2-diphenylvinyl)carbazoles as low cost hole transporting materials for efficient red PhOLEDs, *Dyes and Pigments* (2018), doi: 10.1016/j.dyepig.2018.06.019.

# (Bi)phenyl substituted 9-(2,2-diphenylvinyl)carbazoles as low cost hole transporting materials for efficient red PhOLEDs

Saulius Grigalevicius [a,*], Daiva Tavgeniene [a], Gintare Krucaite [a],
Raimonda Griniene [a], Yen-Po Wang[b], Shang-Ru Tsai [b], Chih-Hao Chang[b,*]

[a] Department of Polymer Chemistry and Technology, Kaunas University of Technology, Radvilenu plentas 19, LT50254, Kaunas, Lithuania

[b] Department of Photonics Engineering, Yuan Ze University, Chung-Li 32003, Taiwan

*****Corresponding authors: Saulius Grigalevicius (saulius.grigalevicius@ktu.lt) and Chih-Hao Chang (chc@saturn.yzu.edu.tw)

**Abstract**

Two low-cost 9-(2,2-diphenylvinyl)carbazole-based derivatives with aryl substitutions were synthesized by simple procedure and then investigated. The respective glass transition temperatures of the materials were estimated to be higher than 90 ℃, which can provide morphologically-stable amorphous films for applications in organic light emitting diodes. The compounds possess adequate ionization potentials and suitable triplet energies, which make them suitable hole transporting materials for use in red phosphorescent organic light-emitting diodes. The respective peak efficiencies of the red devices with the p-type dopants were recorded at 8.7 % (5.6 cd/A and 3.9 lm/W) and at 8.7 % (5.4 cd/A and 3.8 lm/W), correspondingly, demonstrating high potential of the material for applications in light emitting diodes. The characteristics indicated that the devices with the aryl substituted 9-(2,2-diphenylvinyl)carbazoles exhibit better performance than those of widely used hole transporting 1,1-bis[(di-4-tolylamino)phenyl]cyclohexane (TAPC) -based device.

*Keywords:* carbazole derivative, amorphous material, ionization potential, light emitting diode, brightness.

## 1. Introduction

Phosphorescent organic light emitting diodes (PhOLEDs) have attracted much attention because they use both singlet and triplet excitons for generation of light, making 100% internal quantum efficiency possible. Achieving the high level internal quantum efficiency depends on several factors, including high quantum yield emitters, exothermic energy transfer from host to emitter, effective exciton confinement as well as balanced carrier transport [1, 2]. It is well known that carrier transporting materials are crucial to enable a balance carrier transport from cathode and anode [3, 4]. Considerable exertion is needed for the development of efficient red PhOLED devices, because the lower gap of red phosphors usually induces serious carrier trapping, leading to higher operation voltages and carrier imbalance [5]. Accordingly, it is desirable to exploit new hole transport materials to create red PhOLEDs with reduced power consumption and improved efficiency.

Crystallization of low molar mass hole transporting materials during film-formation process and during PhOLEDs operation at high temperature is the main obstacle for their application in the devices [6, 7]. The low glass transition ($T_g$) temperatures lead to the formation of polycrystalline films resulting from thermal stress [8]. It is reported that OLED devices with layers of the widely used commercial hole transporting materials: *N*,*N*,*N'*,*N'*-tetraphenyl-[1,10-biphenyl]-4,4'-diamine (TPD) and *N*,*N'*-diphenyl-*N*,*N'*-bis-(1-naphthyl)-1,1'-biphenyl-4,4'-diamine (NPD) showed irreversible failure when heated above 100 $^{o}$C due to crystallization. The $T_g$ values of organic semiconductors are determined by their molecular structure, i.e. the larger molecular volume results in higher $T_g$ [9, 10].

In this study, the new low cost 9-(2,2-diphenylvinyl)carbazole based derivatives with aryl substitutions were synthesized and investigated. Our previous study found that introducing the diphenylvinyl fragment in carbazole ring could increase spatial hindrance of the moiety and the derivatives could be used for the preparation of thin and stable amorphous layers on substrates [11]. We have examined the novel hole transporting materials in the fabrication of red PhOLEDs. The respective peak efficiencies were recorded at 8.7 % (5.6 cd/A and 3.9 lm/W) and at 8.7 % (5.4 cd/A and 3.8 lm/W), correspondingly, for the devices using 3,6-diphenyl-9-(2,2-diphenylvinyl)carbazole (**6**) and 3-(4-biphenyl)-9-(2,2-diphenylvinyl)carbazole (**7**) as hole transporting materials. The high efficiencies of the red PhOLEDs suggest great potential of the new (2,2-diphenylvinyl)carbazole based electroactive materials for applications in OLED devices.

## 2. Experimental

### *2.1. Instrumentation*

$^1$H NMR spectra were recorded using a Varian Unity Inova (300 MHz) instrument. Mass spectra were obtained on a Waters ZQ 2000 spectrometer. Differential scanning calorimetry (DSC) measurements were carried out using a Bruker Reflex II thermosystem. Thermogravimetric analysis (TGA) was performed on a Netzsch STA 409. TGA and DSC curves were recorded in a nitrogen atmosphere at a heating rate of $10^o$ C/min.

The ionization potentials of the layers of the compounds synthesized were measured in air by the electron photoemission method, which was described earlier [12]. The measurement method was, in principle, similar to that described by Miyamoto et al. [13]. The samples for the ionization potential measurements were prepared as follows [14]. The materials were dissolved in THF and the solution was coated on Al plates pre-coated with ~0.5 μm thick adhesive layer of methylmethacrylate and methacrylic acid copolymer (MKM). The function of this layer was improvement of adhesion as well as elimination of the electron photoemission from Al layer. In addition, the MKM layer was sufficiently conductive to avoid charge accumulation on it during the measurements.

UV-vis spectra of compounds were measured using a Shimadzu UV-1650PC spectrophotometer. The PL spectra of compounds were measured using a CCD spectrograph and the 325 nm line of a He-Cd laser as the excitation source. The hole drift mobility was measured by xerographic time of flight technique [15].

The multilayer phosphorescent devices were fabricated on glass substrates and had the typical structure with the organic layers sandwiched between a bottom indium tin oxide (ITO) anode and a top metal cathode. After routine ultra-sonication cleaning of the ITO-coated glass in deionized water and organic solvents, the substrate was also pre-treated with UV-Ozone for 5 minutes. The organic and metal layers were deposited onto ITO-coated glass by thermal evaporation in a vacuum chamber with a base pressure of $< 10^{-6}$ Torr. Device fabrication was completed in a single cycle without breaking the vacuum. The thicknesses of the organic and metal layers were monitored using an in-situ method by a quartz-crystal microbalance (QCM) equipped in the thermal evaporation chamber. The deposition rates of organic materials and aluminium were respectively kept at around 0.1 nm/s and 0.5 nm/s. The active area was defined by the shadow mask ($2 \times 2$ mm$^2$). Current density-voltage-luminance characteristics were measured using a Keithley 238 current source-measurement unit and a Keithley 6485

pico-ammeter equipped with a calibrated Si-photodiode. The electroluminescent spectra were recorded using an Ocean Optics spectrometer.

*2.2. Materials*

*9H*-Carbazole (**1**), KI, $KIO_3$, 2,2-diphenylacetaldehyde, (±)-camphor-10-sulfonic acid, 4-biphenyl boronic acid, phenyl boronic acid, bis(triphenylphosphine)palladium(II) dichloride ($Pd(PPh_3)_2Cl_2$) and potassium hydroxide were purchased from Aldrich and used as received. 4,4'-*N*,*N'*-dicarbazole biphenyl, 3,5,3',5'-tetra(*m*-pyrid-3-yl)-phenyl[1,1']biphenyl, 1,1-bis[(di-4-tolylamino)phenyl]cyclohexane and tris(1-phenylisoquinoline)iridium(III) were purchased from Lumtec and were subjected to temperature-gradient sublimation before use.

3,6-Diiodo-*9H*-carbazole (**2**) and 3-iodo-*9H*-carbazole (**3**) were obtained by a procedure of Tucker [16].

3,6-Diiodo-9-(2,2-diphenylvinyl)carbazole (**4**) and 3-iodo-9-(2,2-diphenylvinyl)carbazole (**5**) were prepared by earlier described procedure [17].

3,6-Diphenyl-9-(2,2-diphenylvinyl)carbazole (**6**). 3,6-Diiodo-9-(2,2-diphenylvinyl)carbazole (**2,** 0.6 g, 1 mmol), phenyl boronic acid (0.37 g, 3 mmol), $PdCl_2(PPh_3)_2$ (0.042 g, 0.06 mmol) and powdered potassium hydroxide (0.56 g, 10 mmol) were stirred in THF (6 mL) containing degassed water (1 mL) at 80 °C under nitrogen for 24 h. After thin layer chromatography (TLC) control the reaction mixture was cooled and quenched by the addition of ice water. The product was extracted by chloroform. The combined extract was dried over anhydrous $Na_2SO_4$. The crude product was purified by silica gel column chromatography using the mixture of ethyl acetate and hexane (vol. ratio 1:35) as an eluent. Yield: 0.29 g (58 %) of white crystals. M.p.: 220ºC (DSC). MS ($APCI^+$, 20 V): 498.1 ([M+1], 100 %). $^1H$ NMR spectrum ($CDCl_3$, δ, ppm): 8.28 (d, 2H, J = 1.2 Hz); 7.67 (d, 4H, J = 6.9 Hz); 7.53 (d, 2H, J = 1.8 Hz, $J_2$ = 9.0 Hz); 7.50 -7.40 (m, 9H, Ar); 7.31 (t, 2H, J = 7.1 Hz); 7.25 (d, 2H, J = 6.0 Hz); 7.24 (s, 1H, N-C<u>H</u>); 7.14 – 7.06 (m, 5H, Ar). IR (KBr), ($cm^{-1}$) : 3053, 3027 (C-H, Ar); 2951, 2922 (=C-H); 1617, 1599, 1457, 1456 (C=C, Ar); 1357, 1297, 1281 (C-N, Ar); 814 (C-H, >C=CH); 876, 840, 762, 696 (C-H, Ar). Elemental analysis for $C_{38}H_{27}N$ % Calc.: C 91.72, H 5.47, N 2.81; % Found: C 91.69, H 5.44, N 2.83.

3-(4-Biphenyl)-9-(2,2-diphenylvinyl)carbazole (**7**). 3-Iodo-9-(2,2-diphenylvinyl)carbazole (**5,** 0.7 g, 1.5 mmol), 4-biphenyl boronic acid (0.44 g, 2.2 mmol), $PdCl_2(PPh_3)_2$ (0.031 g, 0.044 mmol) and powdered potassium hydroxide (0.41 g, 7.3 mmol) were stirred in THF (7 mL) containing degassed water (1 mL) at 80 °C under nitrogen for 24 h. After TLC control the reaction mixture was cooled and quenched by the addition of ice water. The product was extracted by chloroform. The combined extract was dried over anhydrous $Na_2SO_4$. The crude product was purified by silica gel column chromatography using the mixture of ethyl acetate and hexane (vol. ratio 1:35) as an eluent. Yield: 0.46 g (63 %) of white crystals. M.p.: 188ºC (DSC). MS ($APCI^+$, 20 V): 498.2 ([M+1], 100 %). $^1H$ NMR spectrum ($CDCl_3$, δ, ppm): 8.29 (d, 1H, J = 1.6 Hz); 8.10 (d, 1H, J = 7.6 Hz); 7.77 (d, 2H, J = 8.4 Hz); 7.72 – 7.65 (m, 5H, Ar); 7.59 (dd, 1H, $J_1$ = 1.8 Hz, $J_2$ = 8.6 Hz); 7.51 – 7.22 (m, 12H, Ar); 7.14 – 7.07 (m, 5H, Ar). IR (KBr), ($cm^{-1}$) : 3078, 3051, 3027 (C-H, Ar); 1619, 1598, 1574, 1494 (C=C, Ar); 1355, 1332, 1236, 1231 (C-N, Ar); 828, 846 (C-H, >C=CH); 812, 767, 745, 697 (C-H, Ar). Elemental analysis for $C_{38}H_{27}N$ % Calc.: C 91.72, H 5.47, N 2.81; % Found: C 91.67, H 5.49, N 2.82.

## 3. Results and discussion

The synthesis of phenyl or 4-biphenyl substituted 9-(2,2-diphenylvinyl)carbazole based derivatives (**6** and **7**) was carried out by synthetic route, which is shown in Scheme 1. The key starting compounds: 3,6-diiodo-*9H*-carbazole (**2**) and 3-iodo-*9H*-carbazole (**3**) were synthesized firstly from commercially available *9H*-carbazole (**1**) by Tucker iodination procedure, which is described in the literature [16]. 3,6-Diiodo-9-(2,2-diphenylvinyl)carbazole (**4**) and 3-iodo-9-(2,2-diphenylvinyl)carbazole (**5**) were than prepared in reactions of the iodo-derivatives **1** and **3** with an excess of 2,2-diphenylacetaldehyde under acidic conditions. The objective electroactive materials: 3,6-diphenyl-9-(2,2-diphenylvinyl)carbazole (**6**) and 3-(4-biphenyl)-9-(2,2-diphenylvinyl)carbazole (**7**) were finally synthesized in Suzuki reaction conditions of the intermediates **4** and **5** by using an excess of phenyl boronic acid or biphenyl boronic acid, correspondingly.

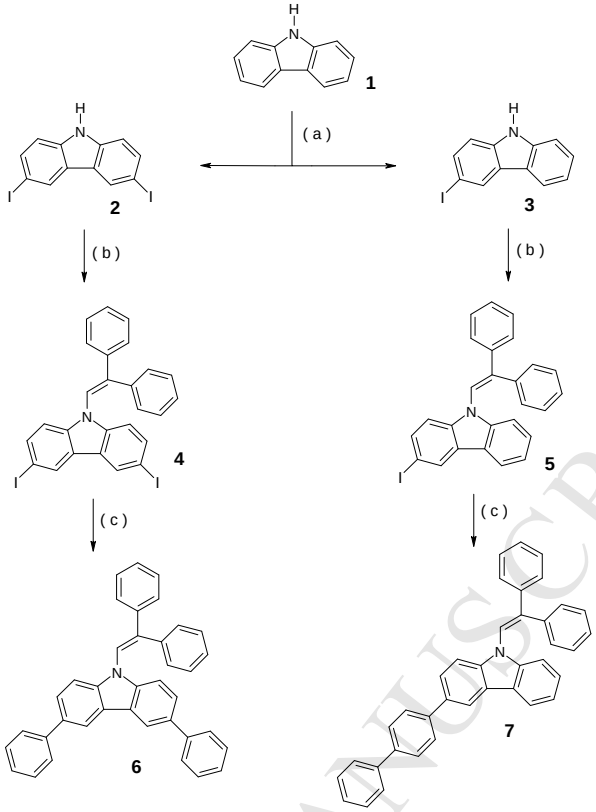


Scheme 1. a) KI, $KIO_3$, acetic acid; b) 2,2-diphenylacetaldehyde, (±)-camphor-10-sulfonic acid, toluene; c) $Pd(PPh_3)_2Cl_2$, KOH, THF, phenyl boronic acid for compound **6** or 4-biphenyl boronic acid for compound **7**.

The synthesized objective derivatives **6** and **7** were identified by mass spectrometry, elemental analysis, infrared (IR) and $^1$H NMR spectroscopy. The data were found to be in good agreement with the proposed structures. The materials were readily soluble in common organic solvents. Transparent thin films of these materials could be prepared by spin coating from solutions or by vacuum evaporation.

The behaviour under heating of the compounds **6** and **7** was investigated by DSC and TGA under a nitrogen atmosphere. It was confirmed by TGA that the materials demonstrate very high thermal stability. The 5 % mass loss was established at 377 $^o$C for **6** and at 392 $^o$C for **7**, as confirmed during the analyses with a heating rate of 10$^o$ C/min.

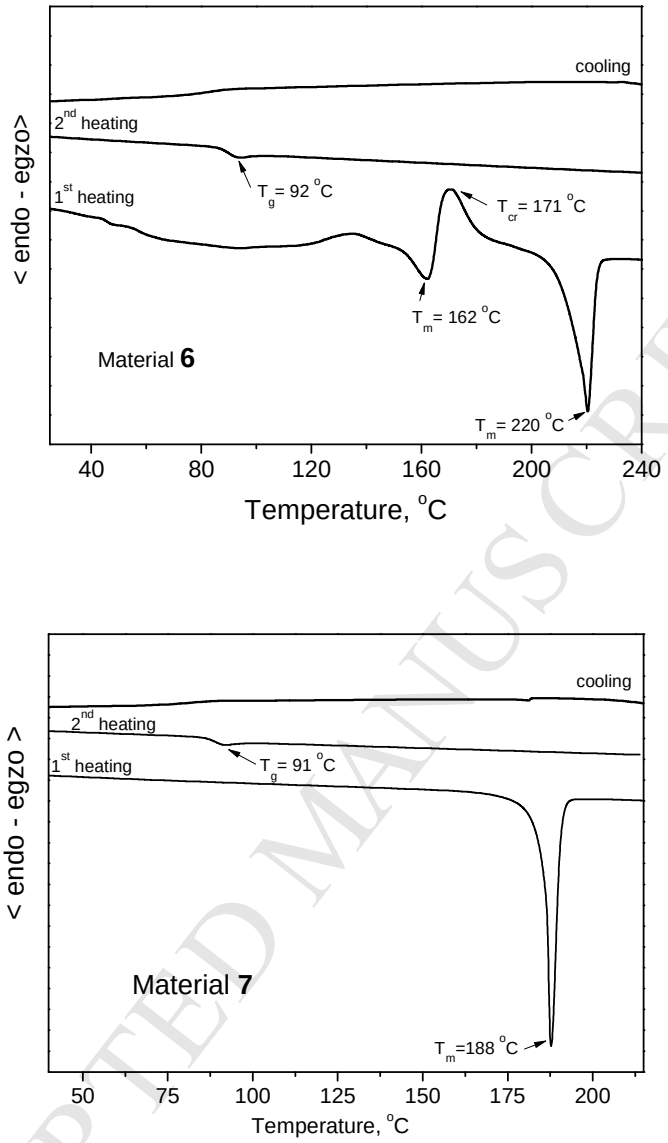


Figure 1. DSC curves of the materials **6** and **7**. Heating rate: 10 °C/min.

Compounds **6** and **7** were obtained as crystalline materials after synthesis; however they could form also amorphous materials with rather high glass transition temperatures ($T_g$) as it was demonstrated by DSC experiment. The DSC thermograms are shown in Figure 1. When the crystalline sample of **6** was heated, first endothermic peak due to melting was observed at 178 °C followed by an exothermic crystallization at 171 °C to obtain new crystals, which melted at 220 °C. When the melted sample was cooled down and heated again, only glass-transition was observed at 92 °C and on further heating no peaks due to crystallization and melting appeared.

Derivative **7** was also obtained after synthesis as crystalline material, however it demonstrated slightly different behaviour in the DSC measurements. The crystalline sample of **7** melted at 188 $^{o}$C on first heating without following crystallization. The melt formed amorphous material upon cooling. When the amorphous sample was heated again, the glass-transition was observed at 91 $^{o}$C and on further heating no peaks due to crystallization and melting appeared. The investigations confirmed that the crystalline derivatives **6** and **7** could be converted into amorphous state and could be used for preparation of thin amorphous layers on substrates.

The ionization potentials ($I_p$) of thin layers of the compounds **6** and **7** were measured by the electron photoemission method. The photoemission spectra of thin amorphous films of these compounds are presented in Figure 2. The values of $I_p$ in eV were 5.75 eV for layer of **6** and 5.7 eV for layer of **7**. It could be observed that biphenyl substituted derivative **7** has a slightly lower value of $I_p$ due to longer conjugated electron system in the molecule. It is also evident that the values of $I_p$ of the newly synthesized compounds **6** and **7** are lower than that of 9-(2,2-diphenylvinyl)carbazole ($I_p$ = 5.94 eV) [18] as well as of derivatives having un-substituted carbazole rings ($I_p$ > 5.9 eV) [19, 20]. The characteristics demonstrate that thin layers of the newly synthesized derivatives could be suitable as hole transporting layer materials for application in optoelectronic devices. The layers should demonstrate better hole-injecting and transporting properties in multilayer electroluminescent devices than that of widely used poly(9-vinylcarbazole) (PVK) [19].

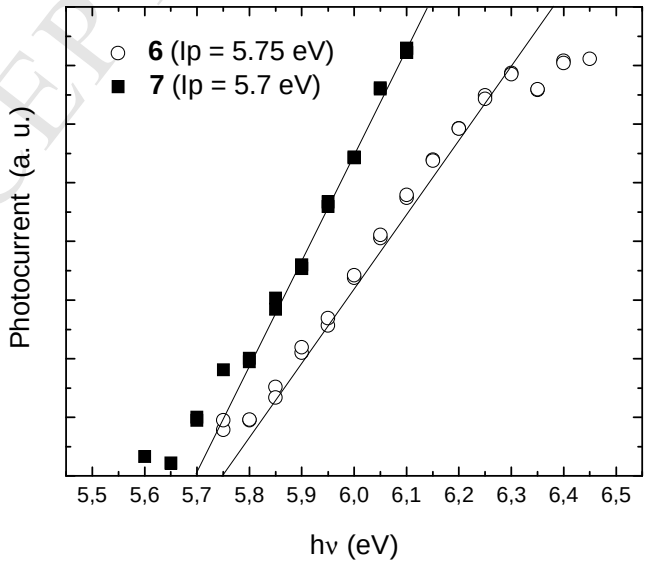


Figure 2. Electron photoemission spectra of layers prepared using the derivatives **6** and **7.**

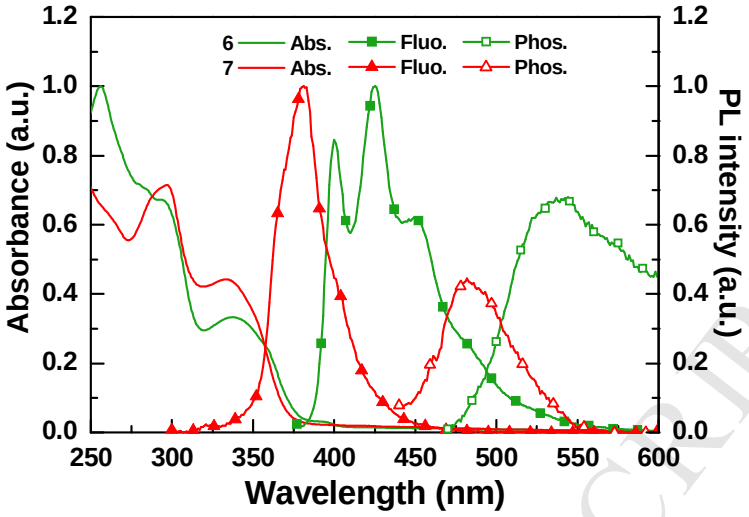


Figure 3. Absorption and fluorescence spectra of the compounds **6** and **7** in hexane at room temperature. Phosphorescence spectra of **6** and **7** in hexane at 77 K.

Table 1. Photo-physical properties of compounds **6** and **7** measured in solutions.

| Material | Absorbance $\lambda_{max.}$ (nm)[a] | Fluo. $\lambda_{peak}$ (nm)[b] | Phos. $\lambda_{peak}$ (nm)[c] | $E_g$ (eV)[d] | $E_T$ (eV)[e] |
|---|---|---|---|---|---|
| **6** | 256, 294, 338 | 400, 425, 449, 482(sh) | 537 | 3.27 | 2.56 |
| **7** | 297, 334 | 369, 381 | 482 | 3.34 | 2.78 |

[a]Absorption maximum; [b]emission peaks of fluorescence; [c]emission peaks of phosphorescence; [d]singlet energy gap ($E_g$) was calculated from the absorption onset; [e]triplet energy gap ($E_T$) was estimated from the phosphorescence onset.

Figure 3 shows absorption spectra, fluorescence spectra, and phosphorescence spectra of compounds **6** and **7** measured in hexane. The respective solution concentrations of compounds **6** and **7** were selected to be 1.0 x $10^{-5}$ M and 8.5 x $10^{-6}$ M for the UV-vis measurements; whereas the respective solution concentrations of compounds **6** and **7** were set to 2.0 x $10^{-5}$ M and 1.7 x $10^{-4}$ M for both fluorescence and phosphorescence. The numeric data of the corresponding photo-physical properties extracted from the figure are also summarized in Table 1. The absorption peaks of both **6** and **7** were similar to those of the carbazole moiety [21]. Nevertheless, the absorption spectral profile of **6** differs slightly from that of **7**, indicating that the different moieties end-capped to the carbazole core influence the Franck-Condon factor and thus alter the absorption intensity. The energy bandgaps calculated from the absorption onset for **6** and **7** are respectively 3.27 and 3.34 eV. On the other hand, both compounds possess quite different fluorescence spectra. The fluorescence of **6** exhibited a

multi-peak spectral profile with clear vibronic features, while **7** possessed a narrower fluorescence spectrum with obscure vibronic peaks. The relatively lower energy gap of **6** implied that the conjugation length was extended as compared to that of the carbazole monomer. The Stoke's shifts of compounds **6** and **7** were estimated to be 61 nm and 35 nm, respectively. The phosphorescence peaks of **6** and **7** measured at 77K were respectively recorded at 537 and 428 nm. Thus, the corresponding triplet energy gaps of **6** and **7** could respectively be determined to be 2.56 eV and 2.78 eV, respectively. The values of triplet energies of **6** and **7** make them both suitable for the use as the hole transport layer (HTL) in red phosphorescent OLEDs [22]. In addition, a widely used hole transport material, 1,1-bis[(di-4-tolylamino)phenyl]cyclohexane (TAPC), possesses an adequate HOMO level of 5.5 eV, a wide triplet energy gap of 2.87 eV, and a high hole mobility of $10^{-2}$ $cm^2/Vs$, and thus could be used as a reference for evaluating the potential of **6** and **7** for EL applications [23]. Herein, we selected phosphorescent $Ir(piq)_3$ as the emitter because its saturated red emission could expand the colour gamut in display applications [ 24 ]. Furthermore, *4,4'-N,N'*-dicarbazolebiphenyl (CBP) with bipolar transport capability was used to combine with the red emitter for constructing an exothermic host-guest system for the emissive layer (EML) [25]. On the other hand, a wide triplet energy gap electron transport material, 3,5,3',5'-tetra(m-pyrid-3-yl)-phenyl[1,1']biphenyl (BP4mPy), was used as the electron transport layer (ETL) due to its high carrier/exciton confinement capability [26]. We constructed the device using a configuration of ITO (120 nm)/ TAPC or **6** or **7** (40 nm)/ CBP doped with 8 wt.% of $Ir(piq)_3$ (30 nm)/ BP4mPy (40 nm)/ LiF (0.8 nm)/ Al (150 nm), where LiF and aluminum were respectively used as the electron injection layer and the reflecting cathode. Figure 4(a) shows a structural drawing of the materials used, while the energy level diagram of the tested OLEDs is shown in Figure 4(b).

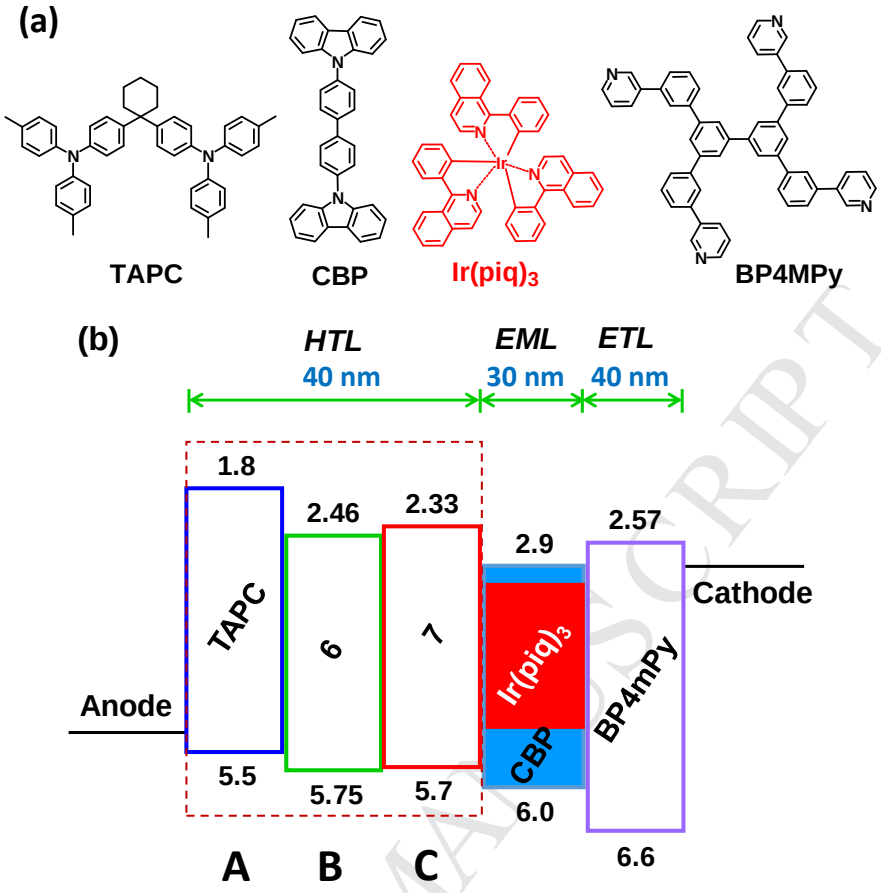


Figure 4. (a) Structural drawings of the materials used in PhOLEDs; (b) energy level diagram of the red phosphorescent OLEDs with different HTLs.

Figure 5 and Table 2, respectively, provide the EL characteristics and the corresponding numeric data of the tested red phosphorescent OLEDs. Figure 5(a) shows the normalized EL spectra of devices A, B and C measured at 100 cd/m$^2$. All the devices presented an identical spectral profile of Ir(piq)$_3$, indicating that the doping concentration of the emitter was appropriate and the exciton formation zone was located within the EML [27]. Moreover, no additional emission peak was observed in the EL spectra, implying that both **6** and **7** could provide effective exciton confinement like TAPC. Thus, the tested devices with the pure Ir(piq)$_3$ saturated red emission resulted in the corresponding CIE coordinates being superimposed on the NTSC vertices. In addition, almost no color variation occurred as the voltage increased, verifying the thermal stability of these newly developed hole transport materials for EL applications.

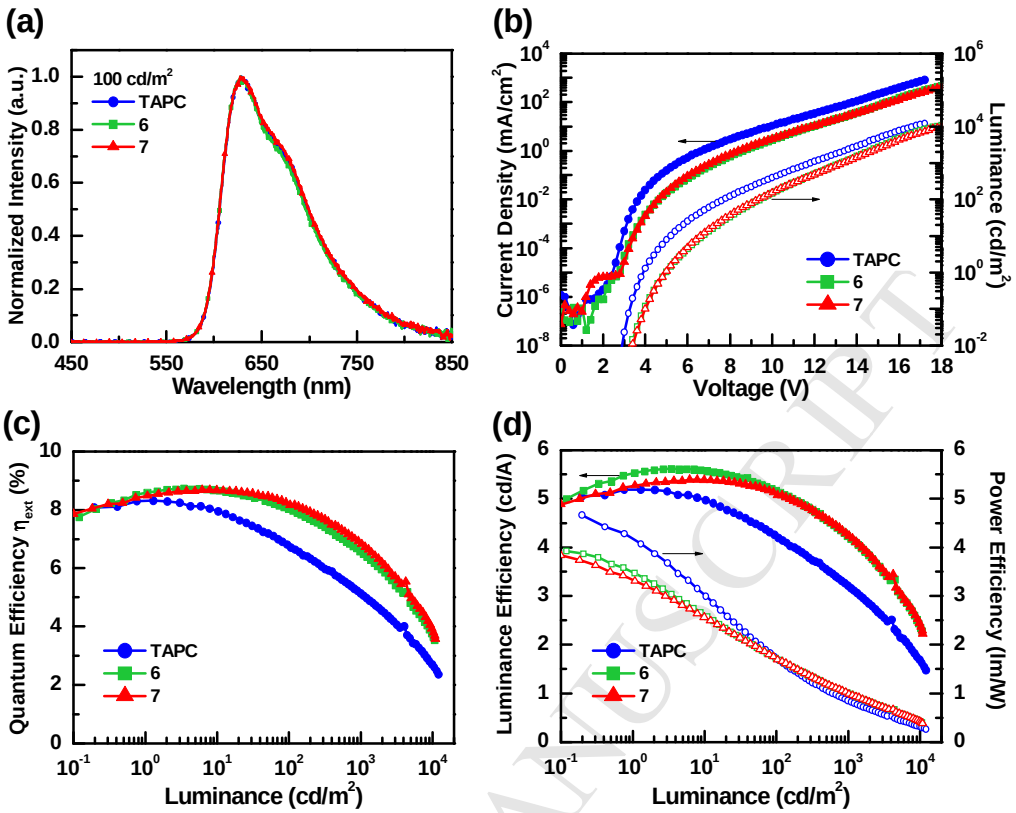


Figure 5. EL characteristics of the red phosphorescent OLEDs: (a) normalized EL spectra; (b) current density-voltage-luminance (*J*-*V*-*L*) curves; (c) external quantum efficiency vs luminance; (d) luminance efficiency and power efficiency of devices A, B, and C.

Table 2. EL Characteristics of red phosphorescent OLEDs with different HTLs.

| **Device** | | **A** | **B** | **C** |
|---|---|---|---|---|
| **HTL** | | **TAPC** | **6** | **7** |
| External Quantum Efficiency (%) | Max. | 8.3 | 8.7 | 8.7 |
| | 100 cd/m$^2$ | 6.8 | 8.0 | 8.2 |
| | 1000 cd/m$^2$ | 5.1 | 6.6 | 6.9 |
| Luminance Efficiency (cd/A) | Max. | 5.2 | 5.6 | 5.4 |
| | 100 cd/m$^2$ | 4.2 | 5.2 | 5.1 |
| | 1000 cd/m$^2$ | 3.2 | 4.2 | 4.3 |
| Power Efficiency (lm/W) | Max. | 4.7 | 3.9 | 3.8 |
| | 100 cd/m$^2$ | 1.7 | 1.7 | 1.7 |
| | 1000 cd/m$^2$ | 0.9 | 1.0 | 1.0 |
| Turn-on voltage (V) | 1 cd/m$^2$ | 3.9 | 5.0 | 5.0 |
| Max. Luminance (cd/m$^2$) [V] | | 12223 [17.2] | 10740 [18.0] | 10951 [18.6] |
| CIE coordinates (x, y) | 100 cd/m$^2$ | (0.682, 0.316) | (0.682, 0.317) | (0.682, 0.316) |
| | 1000 cd/m$^2$ | (0.681, 0.316) | (0.682, 0.317) | (0.682, 0.317) |

As shown in the current density-voltage-luminance (*J-V-L*) curves (Figure 5(b)), device A with TAPC exhibited a higher current density than devices B and C, due to the lower hole mobilities of **6** and **7**. Furthermore, comparing the HOMO level of TAPC, the slightly higher HOMO levels of **6** and **7** produced higher energy barriers at the HTL/EML interface and thus obstructed hole injection into the EML. Hence, the turn-on voltages of both devices B and C were recorded at 5.0 V, while device A exhibited lower value of 3.9 V. Similarly, the maximum luminance of devices A, B, and C was respectively recorded at 12223, 10740, and 10951 cd/m$^2$.

The efficiency curves of the tested devices are shown in Figures. 5(c) and 5(d). As indicated, devices B and C presented similar external quantum efficiency and luminance efficiency curves, and were both higher than those of device A. The respective maximum efficiencies of devices B and C were respectively recorded at 8.7 % (5.6 cd/A and 3.9 lm/W) and 8.7 % (5.4 cd/A and 3.8 lm/W), while device A achieved a peak efficiency of 8.3% (5.2 cd/A and 4.7 lm/W). In addition, the efficiency curve of device A achieved a peak value in a low luminance range and decreased immediately thereafter. Significant efficiency roll-off was observed in

device A, possibly due to the serious triplet-triplet annihilation (TTA) [28]. At more practical luminance values of 100 cd/m$^2$ and 1000 cd/m$^2$, device A only gave external quantum efficiencies of 6.8% and 5.1%, respectively. In contrast, at a luminance of 100 cd/m$^2$ (1000 cd/m$^2$), devices B and C maintained higher efficiency values, with corresponding forward efficiencies of 8.0% (6.6%) and 8.2% (6.9%). The different tendencies of the carrier balance between devices was due to the difference in hole mobility and the energy barrier at the HTL/EML interface, leading to different exciton formation zone location and size in the EML. Since the electron mobility of BP4mPy was estimated to be about $10^{-4}$ cm$^2$/V·s, both **6** and **7** possessed adequate hole mobility and could match BP4mPy, providing carrier balance in a broad luminance range [27]. At an electric field of $4\times10^5$ V/cm, hole mobility value of $4.5\times10^{-4}$ cm$^2$/(V·s) was obtained for compound **6**, while slightly lower hole mobility value of $2\times10^{-4}$ cm$^2$/(V·s) was obtained for the compound **7** as it was demonstrated by time of flight measurements. In addition, one could expect an enlarged exciton formation zone achieved in devices B and C, which could mitigate the TTA. Furthermore, the HOMO levels of either **6** or **7** were close to that of the EML, preventing hole accumulation at the HTL/EML interface and thus mitigating the polaron quenching. As the result, efficiency drops from the peak to the value recorded at a luminance level of 1000 cd/m$^2$ for devices B and C were only estimated to be 24% and 21%, respectively. Overall, the outcome indicated that the simple tri-layer architecture device incorporating **6** or **7** rendered very good performance with high luminance levels and demonstrated the high potential of these fabricated hole transport materials.

## 4. Conclusions

New low-cost aryl substituted 9-(2,2-diphenylvinyl)carbazole-based derivatives aiming to facilitate hole transport function in phosphorescent organic light emitting diodes were synthesized and investigated. The electroluminescent characteristics of the tested OLEDs indicated that devices with layers of the new hole transporting materials exhibited better efficiencies to that of commercially available 1,1-bis[(di-4-tolylamino)phenyl]cyclohexane (TAPC)-based device. By introducing new p-type 3,6-diphenyl-9-(2,2-diphenylvinyl)carbazole (**6**) for hole transporting layer, the respective peak efficiency of a red phosphorescent organic light emitting diode was respectively recorded at 8.7 % (5.6 cd/A and 3.9 lm/W) and at 8.0 % (5.2 cd/A and 1.7 lm/W) for 100 cd/m$^2$ brightness. By introducing hole transporting layer of 3-(4-biphenyl)-9-(2,2-diphenylvinyl)carbazole (**7**), the peak efficiency of the analogues device

was 8.7 % (5.4 cd/A and 3.8 lm/W) and 8.2 % (5.1 cd/A and 1.7 lm/W) for 100 cd/m$^2$ brightness. The good results of the devices with the aryl substituted 9-(2,2-diphenylvinyl)carbazoles indicated a new path of molecular designs for the hole transporting materials for the red phosphorescent organic light emitting diodes.

**Acknowledgements**

This research was funded by a grant No. S-MIP-17-64 from the Research Council of Lithuania. Prof. C.-H. Chang gratefully acknowledge financial support from the Ministry of Science and Technology of Taiwan (MOST 106-2221-E-155-035-). Dr. habil. Valentas Gaidelis is acknowledged for measurements of electronic properties of layers of the material.

**References**

[1] C.-H. Chang, C.-L. Ho, Y.-S. Chang, I-C. Lien, C.-H. Lin, Y.-W. Yang, J.-L. Liao, Y. Chi, J. Mater. Chem. C, 1 (2013) 2639.

[2] J. Huang, B. Xu, J.H. Su, C.H. Chen, H. Tian, Tetrahedron. 66 (2010) 7577.

[3] J. Huang, J.H. Su, H. Tian, J. Mater. Chem. 22 (2012) 10977.

[4] C. W. Lee, J. Y. Lee, Organic Electronics 15 (2014) 399.

[5] C.-H. Chang, Y.-H. Lin, C.-C. Wu, L.-S. Chen, W.-W. Wu, Y. Chi, Org. Electron. 10 (2009) 1235.

[6] J. W. Kingsley, P. P. Marchisio, H. Yi, A. Iraqi, C. J. Kinane, S. Langridge, R. L. Thompson, A. J. Cadby, A. J. Pearson, D. G. Lidzey, R. A. L. Jones and A. J. Parnell, Sci. Rep., 4 (2014) 5286.

[7] Z. Y. Xiao, K. Sun, J. Subbiah, T. S. Qin, S. R. Lu, B. Purushothaman, D. J. Jones, A. B. Holmes and W. W. H. Wong, Polym. Chem., 6 (2015) 2312.

[8] D. E. Loy, B. E. Koene and M. E. Thompson, Adv. Funct. Mater., 12 (2002) 245.

[9] S. Feng, L. Duan, L. D. Hou, J. Qiao, D. Q. Zhang, G. F. Dong, L. D. Wang and Y. Qiu, J. Phys. Chem. C, 115 (2011) 14278.

[10] M. Nagai and H. Nozoye, J. Electrochem. Soc., 154 (2007) J239.

[ 11 ] R. Griniene, J.V. Grazulevicius, K.Y. Tseng, W.B. Wang, J.H. Jou, S. Grigalevicius, Synthetic Metals 161 (2011) 2466.

[12] M. Kirkus, R. Lygaitis, M.-H. Tsai, J.V. Grazulevicius, C.-C. Wu, Synthetic Metals 158 (2008) 226.

[13] E. Miyamoto, Y. Yamaguchi, M. Yokoyama, Electrophotography 28 (1989) 364.

[14] A. Balionyte, E. Lideikis, S. Grigalevicius, J. Ostrauskaite, E. Burbulis, V. Jankauskas, E. Montrimas, J.V. Grazulevicius, J. Photochem. Photobiol. A: Chem. 162 (2004) 187.

[15] S. M. Vaezi-Nejad, Int. J. Electron. 62 (1987) 361–384.

[16] S. H.Tucker, J. Chem. Soc. 1 (1926) 548.

[17] R. Griniene, J.V. Grazulevicius, K.Y. Tseng, W.B. Wang, J.H. Jou, S. Grigalevicius, Synthetic Metals 161 (2011) 2466.

[18] A. Matoliukstyte, E. Burbulis, J.V. Grazulevicius, V. Gaidelis, V. Jankauskas, Synthetic Metals 158 (2008) 462.

[19] P. Strohriegl, J.V. Grazulevicius, J. Pielichowski, K. Pielichowski, Prog. Polym. Sci. 28 (2003) 1297.

[20] R. Stanionyte, G. Buika, J. V. Grazulevicius, S. Grigalevicius, Polym Int. 57 (2008) 1036.

[21] M.-H. Tsai, H.-W. Lin, H.-C. Su, T.-H. Ke, C.-C. Wu, F.-C. Fang, Y.-L. Liao, K.-T. Wong, C.-I Wu, Adv. Mater. 18 (2006) 1216.

[22] C.-H. Chang, G. Krucaite, D. Lo, Y.-L. Chen, C.-C. Su, T.-C. Lin, J. V. Grazulevicius, L. Peciulyte, S. Grigalevicius, Dyes and Pigments 136 (2017) 302.

[23] N. Chopra, J. Lee, Y. Zheng, S.-H. Eom, J. Xue, F. So, Appl. Phys. Lett. 93 (2008) 143307.

[24] A. Tsuboyama, H. Iwawaki, M. Furugori, T. Mukaide, J. Kamatani, S. Igawa, T. Moriyama, S. Miura, T. Takiguchi, S. Okada, M. Hoshino, K. Ueno, J. Am. Chem. Soc. 125 (2003) 12971.

[25] D. F. O'Brien, M. A. Baldo, M. E. Thompson, S. R. Forrest, Appl. Phys. Lett. 74 (1999) 442.

[26] S.-J. Su, D. Tanaka, Y.-J. Li, H. Sasabe, T. Takeda, J. Kido, Org. Lett. 10 (2008) 941.

[27] C.-H. Chang, C.-L. Ho, Y.-S. Chang, I-C. Lien, C.-H. Lin, Y.-W. Yang, J.-L. Liao, Y. Chi, J. Mater. Chem. C 1 (2013) 2639.

[28] M. A. Baldo, C. Adachi, S. R. Forrest, Phys. Rev. B 62 (2000) 10967.

9-(2,2-diphenylvinyl)carbazole based hole transporting materials with aryl substitutions were synthesized.

The hole transporting materials possess adequate ionization potentials and triplet energies.

Red PhOLEDs using the hole transporting materials were formed.

Peak external quantum efficiencies of the devices reached 8.7 %